

Guiding Stem Cell Differentiation into Oligodendrocytes Using Graphene-Nanofiber Hybrid Scaffolds

Shreyas Shah, Perry T. Yin, Thiers M. Uehara, Sy-Tsong Dean Chueng, Letao Yang, and Ki-Bum Lee*

Damage to the central nervous system (CNS) from degenerative diseases or traumatic injuries is particularly devastating due to the limited regenerative capabilities of the CNS. Among the current approaches, stem-cell-based regenerative medicine has shown great promise in achieving significant functional recovery by taking advantage of the self-renewal and differentiation capabilities of stem cells, which include pluripotent stem cells (PSCs), mesenchymal stem cells (MSCs) and neural stem cells (NSCs).^[1] However, the low survival rate upon transplantation has been a longstanding barrier for scientists and clinicians to overcome.^[2] To this end, numerous types of natural and synthetic biomaterial scaffolds have been developed, the two main classes being hydrogels and nanofibers, in an attempt to mimic the cellular microenvironment, support cellular growth and improve cellular viability.^[3] Nevertheless, designing scaffolds with defined properties to selectively guide stem cell differentiation towards a specific neural cell lineage is still an ongoing challenge.

For CNS regeneration, the selective differentiation of NSCs into either neurons or oligodendrocytes (as opposed to astrocytes) is highly desirable.^[4] A number of approaches have been employed to guide differentiation into neurons, including genetic modifications, growth factors, cytokines, substrate topography and even nanomaterials.^[5] However, oligodendrocyte differentiation has proven to be much more elusive, resulting in only a small percentage of the differentiated cell population.^[6] The primary approach to guide oligodendrocyte differentiation has focused on either developing culture media containing a combination of growth factors or the forced expression of key oligodendrocyte-promoting transcription factors via viral gene transfection.^[7] However, developing a biomaterials-approach to achieve efficient differentiation of NSCs into mature oligodendrocytes, which are the myelinating cells

of the CNS, while eliminating the potential adverse or variable side-effects from growth factors and viral gene vectors, would be highly beneficial.^[8]

Herein, we report the use of a graphene-based nanomaterial for the design of hybrid nanofibrous scaffolds to guide NSC differentiation into oligodendrocytes (**Figure 1**). Graphene-based nanomaterials, such as graphene oxide (GO), have recently gained considerable interest for tissue engineering applications due to their favorable chemical, electrical and mechanical properties.^[9] Besides serving as a highly elastic and flexible structural reinforcement, substrates coated with GO have been demonstrated to promote the growth and differentiation of various stem cell lines, including induced PSCs, MSCs and NSCs.^[10] Based on these considerations, we demonstrate the use of GO as an effective coating material in combination with electrospun nanofibers for the selective differentiation of NSCs into oligodendrocytes. By varying the amount of GO coating on the nanofibers, we observed a GO concentration-dependent change in the expression of key neural markers, wherein coating with a higher concentration of GO was seen to promote differentiation into mature oligodendrocytes. Further investigation into the role of GO-coating on the nanofibrous scaffolds showed the overexpression of a number of key integrin-related intracellular signaling molecules that are known to promote oligodendrocyte differentiation in normal development.

Electrospun nanofiber scaffolds exhibit several key properties that are advantageous for neural tissue engineering, including a high degree of porosity, high surface-to-volume ratio, and a relatively close structural mimic of the native extracellular matrix (ECM).^[11] From the wide array of polymeric materials available, we used polycaprolactone (PCL) to generate our nanofibrous scaffolds. PCL is a biodegradable and biocompatible polyester approved by the FDA for use in the human body as a drug delivery device and suture, and is also widely used for neural tissue engineering.^[12] In our studies, PCL was electrospun onto a metallic collector and then transferred to glass substrates for cell culture using a medical grade adhesive. Nanofibers with an average diameter of 200–300 nm were generated, which is a fiber size range that has been reported to be favorable for oligodendrocyte culture, potentially due to the close morphological resemblance to axons^[13] (**Figure 2a**). Thin-layered graphene oxide (GO) was then synthesized and dispersed in deionized water (**Figure S1**, Supporting Information). The hydrophobic PCL nanofibers were exposed to oxygen plasma to render the surface hydrophilic (**Figure S2**, Supporting Information). The GO was then deposited on the PCL nanofiber surface, thus allowing for the efficient and uniform coating of the PCL nanofiber surface with GO, as seen

S. Shah, S.-T. D. Chueng, L. Yang, Prof. K.-B. Lee
Department of Chemistry
and Chemical Biology, Rutgers
The State University of New Jersey
Piscataway, NJ 08854, USA
E-mail: kblee@rutgers.edu

P. T. Yin, Prof. K.-B. Lee
Department of Biomedical Engineering
Rutgers, State University of New Jersey
Piscataway, NJ 08854, USA

T. M. Uehara
Physics Institute of São Carlos
University of São Paulo
CP 369 São Carlos, São Paulo 13566, Brazil



DOI: 10.1002/adma.201400523

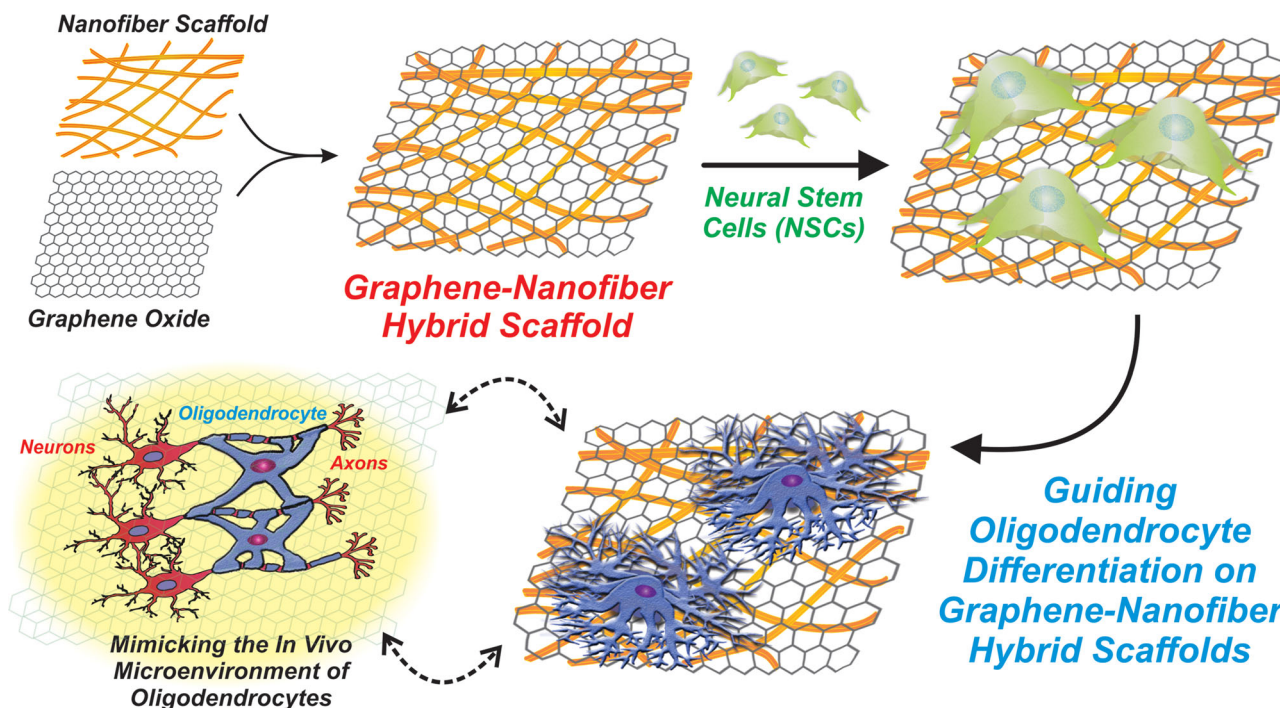


Figure 1. Schematic diagram depicting the fabrication and application of graphene-nanofiber hybrid scaffolds. Polymeric nanofibers (composed of polycaprolactone) generated using electrospinning were subsequently coated with graphene oxide (GO) and seeded with neural stem cells (NSCs). NSCs cultured on the graphene-nanofiber hybrid scaffolds show enhanced differentiation into oligodendrocyte lineage cells.

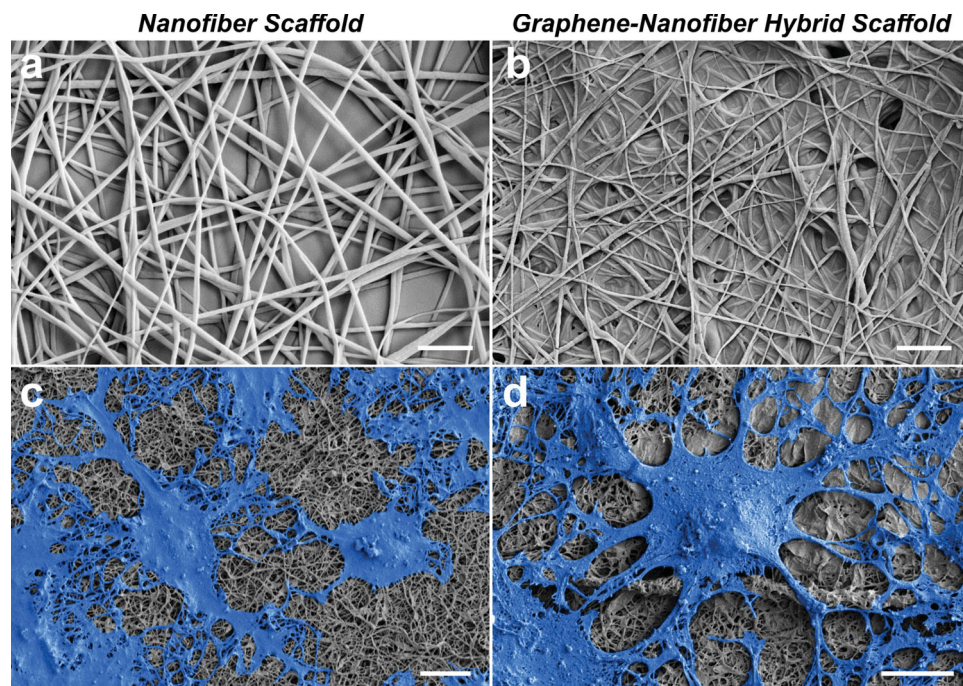


Figure 2. Morphology of nanofibrous scaffolds and cultured NSCs on the scaffolds. a,b) FE-SEM images of PCL nanofibers (a) and PCL nanofibers coated with GO using 1.0 mg/mL GO solution (b). Scale bars: 2 μm . c,d) FE-SEM of differentiated NSCs cultured on PCL nanofiber scaffolds (c) and graphene-nanofiber hybrid scaffolds (d) after six days of culture. The cells are pseudo-colored blue for contrast. The differentiated cells on the graphene-nanofiber hybrid scaffolds (d) show a clear morphological difference in terms of process extension compared with the nanofiber scaffolds alone (c). Scale bars: 10 μm .

with field emission scanning electron microscopy (FE-SEM) (Figure 2b and Figure S3, Supporting Information) and helium ion microscopy (Figure S4, Supporting Information).

For the culture of NSCs, the scaffolds were then coated with laminin, a well-established ECM protein which is essential for the adhesion, growth and differentiation of NSCs.^[14] Green fluorescent protein-labeled adult rat hippocampal NSCs (purchased from Millipore) were then seeded onto the scaffolds and the morphology was monitored using fluorescence microscopy. After six days of culture, a significant difference in the cellular morphology was evident on GO-coated nanofibers compared to the nanofibers alone (Figure S5, Supporting Information). FE-SEM shows cell attachment on these surfaces in greater detail, wherein the cells on the GO-coated nanofibers display extensive branching of cell processes (Figure 2c,d and Figure S6, Supporting Information). This type of extensive process extension is a characteristic attribute reported to distinguish oligodendrocytes from other neural cells.^[15] This difference in cellular morphology provides evidence for the potential

ability of our hybrid scaffolds to enhance NSC differentiation into oligodendrocytes.

To systematically investigate the effect of GO-coating on NSC differentiation, we generated hybrid scaffolds with varying amounts of GO-coating. Solutions containing three different concentrations of GO (0.1, 0.5 and 1.0 mg/mL) were deposited on oxygen plasma-treated PCL nanofibers. The degree of coating using the various GO concentrations was then observed using FE-SEM (Figure 3a). GO-coating of PCL with 0.1 mg/mL, indicated as PCL-GO (0.1), shows the clear presence of GO compared with the PCL nanofibers alone, with uniform coating on the surface of individual fibers. In contrast, PCL-GO (0.5) and PCL-GO (1.0) exhibit a much greater extent of GO attachment on the nanofibrous surface, showing a high degree of GO coating and connectivity between fibers. This was confirmed quantitatively using Raman spectroscopy, where the characteristic peaks of the D band (ca. 1350 cm^{-1}) and G band (ca. 1600 cm^{-1}) indicate the presence of GO. Comparison of the Raman intensity of these peaks further supports

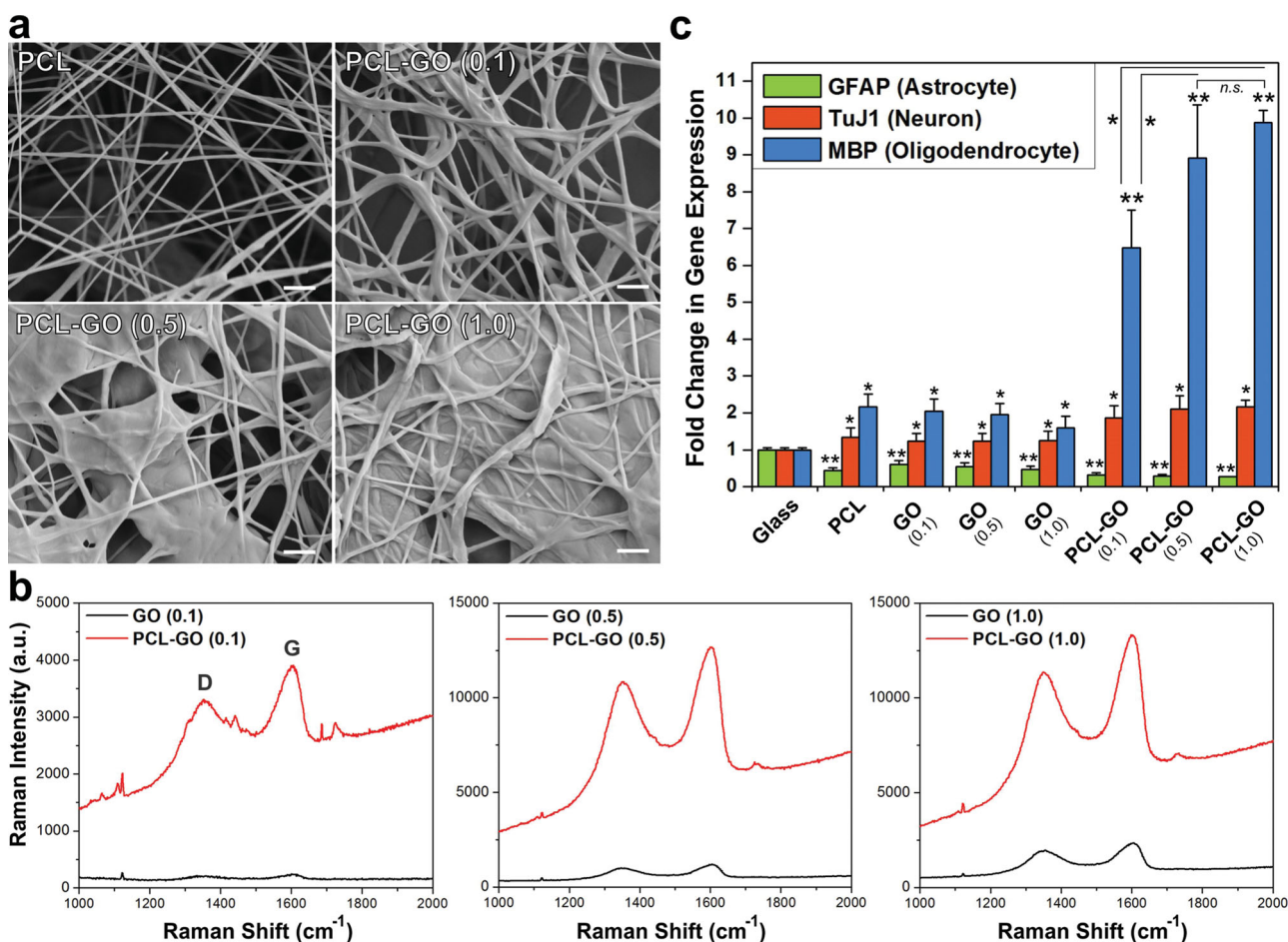


Figure 3. Effect of concentration-dependent GO-coating on NSC differentiation. a) FE-SEM images of PCL nanofibers coated with GO solutions of varying concentrations: 0.0 mg/mL [PCL], 0.1 mg/mL [PCL-GO (0.1)], 0.5 mg/mL [PCL-GO (0.5)] and 1.0 mg/mL [PCL-GO (1.0)]. Scale bars: 1 μm . b) Raman spectroscopy of glass and PCL nanofibers coated with varying concentrations of GO. c) Quantitative PCR of NSCs grown on various substrates from RNA isolated after six days of culture. The plot shows fold change in gene expression of markers indicative of neurons (TuJ1), astrocytes (GFAP) and oligodendrocytes (MBP), wherein the PCL-GO substrates show the highest expression of MBP. The gene expression is relative to GAPDH, and normalized to the conventional PLL-coated glass control. Student's unpaired t-test was used for evaluating significance (* = $p < 0.05$, ** = $p < 0.01$, n.s. = no significance), compared to the PLL-coated glass control (denoted above the bar) or between different substrates.

the trend described above in terms of concentration-dependent GO coating on the PCL nanofiber surfaces (Figure 3b). Moreover, the nanofibrous scaffolds at all three concentrations show significantly higher GO content compared with the control glass surfaces coated with the same respective amounts of GO (Figure 3b). The higher surface area-to-volume of the nanofibers available for GO attachment, in conjunction with the 3D structure of these scaffolds, may attribute to this difference in coating.

These various PCL-GO substrates were then used to examine the influence of GO-coating on modulating NSC differentiation. For comparison, the following control substrates were used: i) PLL-coated glass (conventional substrate for *in vitro* neural cultures), ii) PCL nanofibers alone, and iii) GO-coated glass (at the abovementioned three GO concentrations). All of the substrates were coated with laminin to facilitate NSC attachment, and the cells were harvested after six days of culture to compare the gene expression of key neural markers. Quantitative PCR (qPCR) was utilized to compare gene expression of three key markers that are indicative of differentiated NSCs: glial fibrillary acidic protein (GFAP; astrocytes), beta-III tubulin (TuJ1; neurons) and myelin basic protein (MBP; mature oligodendrocytes). First, it is important to note that both the PCL nanofibers alone and GO-coated glass (at all three concentrations) individually show enhanced oligodendrocyte gene expression, with about a 2-fold increase in MBP expression (Figure 3c). At the same time, TuJ1 shows only about a 1.3-fold increase and GFAP shows about a 0.5-fold decrease in expression, which indicates a stronger preference for differentiation towards oligodendrocytes rather than neurons and astrocytes (Figure 3c). While no reports exist for the effect of graphene-based nanomaterials on oligodendrocyte differentiation, previous studies have reported that electrospun nanofibers can act as permissive culture platforms for oligodendrocyte culture.^[16]

Since each individual component (nanofibers and GO) displayed a favorable trend in NSC differentiation towards oligodendrocytes, we hypothesized that the combination of GO and nanofibers in a single scaffold may have a synergistic effect. In the PCL-GO samples, we observed a remarkable trend in gene expression of these neural markers. The nanofibers coated at the lowest GO concentration (0.1 mg/mL) showed a 6.5-fold increase in MBP, which is much higher than the expression on PCL nanofibers alone and GO-coated glass controls (Figure 3c). Interestingly, this enhancement in MBP expression was even more pronounced when the concentration of GO was further increased, wherein the cells on PCL-GO (0.5) showed an 8.9-fold increase and PCL-GO (1.0) showed a 9.9-fold increase in MBP expression (Figure 3c). Based on the data, there is no statistically significant difference in MBP expression on the PCL-GO (0.5) and PCL-GO (1.0), indicating the saturation of GO on the PCL nanofiber surface. The overall increase in MBP expression of the cells grown on the PCL-GO substrates points to the role of GO in the observed result, in which the 3D PCL nanotopography serves to increase the amount of GO coating and the consequent surface interface in contact with the NSCs compared with the traditional 2D surfaces. In addition, the simultaneous decrease in GFAP expression and relatively small increase in TuJ1 expression provides further evidence that the hybrid scaffold promotes selective NSC differentiation, with a strong

preference towards oligodendrocyte lineage cells (Figure 3c). To explore the potential of these hybrid scaffolds as a culture platform for oligodendrocyte differentiation, we elected to use PCL-GO (1.0) for all subsequent experiments (termed PCL-GO hereafter). In regard to biocompatibility, NSCs grown on these scaffolds show excellent survival, as found with cell viability assays (Figure S7, Supporting Information).

We next sought to further characterize the degree of differentiation into oligodendrocytes by examining the expression of well-established oligodendrocyte markers at the genetic and cellular-level. After six days of culture, the cells grown on PCL-GO were immunostained for the early marker Olig2 and the mature marker MBP (Figure 4a,b). The immunostained cells show extensive expression of both the nuclear-localized Olig2 and the cytosolic MBP. A similar expression was also observed for the oligodendrocyte-specific surface markers O4 (early) and GalC (mature) (Figure S8, Supporting Information). Expression of these protein markers confirms the successful NSC differentiation into oligodendrocytes. The degree of differentiation was further quantified by determining the percentage of cells expressing Olig2 and MBP on the various substrates (Figure 4c,d). While the conventional PLL-coated glass substrates showed only about 9% of the cells expressing Olig2, both the PCL only and GO-coated glass substrates showed about 16% Olig2-expressing cells (Figure 4c). On the other hand, the PCL-GO substrate displayed about 33% of the cells expressing Olig2, which is significantly higher than all other conditions (Figure 4c). A similar trend was also observed for MBP expression, wherein 26% of the cells on PCL-GO were positive for MBP, which corroborates the gene expression results shown earlier (Figure 3c). Comparison of the percentage of cells stained for TuJ1 (neurons) and GFAP (astrocytes) further supports the selective differentiation into oligodendrocytes, with PCL-GO displaying a significant decrease in GFAP-positive cells and a minor increase in the number of TuJ1-positive cells (Figure S9, Supporting Information). Given the difficulty in achieving the spontaneous differentiation of stem cells into oligodendrocytes, our unique graphene-nanofiber hybrid scaffolds exhibit a significant enhancement in oligodendrocyte formation.

To further confirm that the hybrid scaffolds promote oligodendrocyte differentiation, we evaluated changes in gene expression for a variety of well-known early and mature oligodendrocyte-specific markers. qPCR was carried out for detecting the gene expression of: i) early markers including 2',3'-cyclic-nucleotide 3'-phosphodiesterase (CNP), platelet-derived growth factor receptor alpha (PDGFR α), Olig1 and Olig2, and ii) mature markers including proteolipid protein (PLP), MBP, myelin-associated glycoprotein (MAG), myelin oligodendrocyte glycoprotein (MOG), adenomatous polyposis coli (APC), glutathione S-transferase-pi (GST- π) and galactocerebroside (GalC). For all genes of interest, NSCs on PCL-GO exhibited the strongest level of expression compared with all other control substrates (Figure 4e,f and Figure S10, Supporting Information). Interestingly, several of the known genes indicative of myelinating oligodendrocytes also showed a substantial increase in gene expression. For instance, MAG and MOG, which are glycoproteins reported to be crucial during the myelination process in the CNS,^[15] were seen to have a 17-fold and

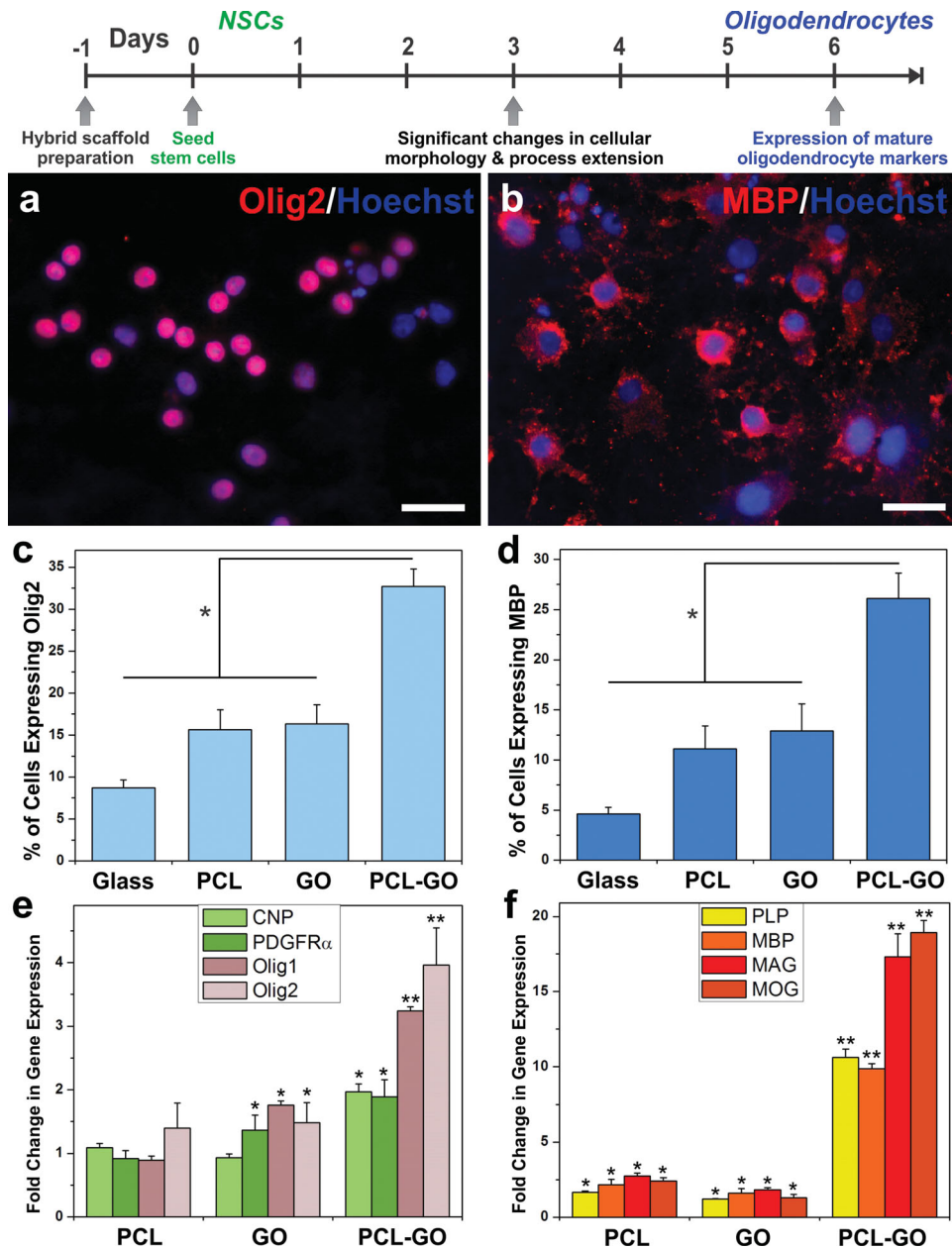


Figure 4. Enhancement in oligodendrocyte differentiation on PCL-GO. a,b) Fluorescence image of NSCs grown on PCL-GO after six days of culture, stained for the early oligodendrocyte marker Olig2 (a) and the mature oligodendrocyte marker MBP (b). Scale bars: 20 μm . c,d) Quantitative comparison on various substrates of the percentage of cells expressing Olig2 (c) and MBP (d). The graphs show the mean \pm s.e.m, $n = 3$, comparison by ANOVA – * = $p < 0.01$. e,f) Quantitative PCR analysis was used to assess the gene expression of early oligodendrocyte markers including CNP, PDGFR α , Olig1 and Olig2 (e), and mature oligodendrocyte markers including PLP, MBP, MAG and MOG (f). The gene expression is relative to GAPDH, and normalized to the conventional PLL-coated glass control. A student's unpaired t-test was used for evaluating the significance (* = $p < 0.05$, ** = $p < 0.01$), compared to the PLL-coated glass control.

19-fold increase in gene expression, respectively (Figure 4f). Taken together, these results confirm that NSCs cultured on PCL-GO substrates exhibit a strong preference towards oligodendrocyte differentiation.

These hybrid scaffolds provide a unique microenvironment that was found to be permissive to oligodendrocyte formation. Nevertheless, how the extracellular cues from these hybrid scaffolds modulate intracellular signaling pathways to control this

selective differentiation remains to be explored. Numerous studies report the importance of stem cell–extracellular matrix interactions in directing oligodendrocyte differentiation.^[17] These interactions have been observed to modulate intracellular signaling pathways, primarily through the activation of integrin receptors found on the cellular membrane. Integrin-mediated signaling has been found to be especially important for facilitating fundamental oligodendrocyte processes, such

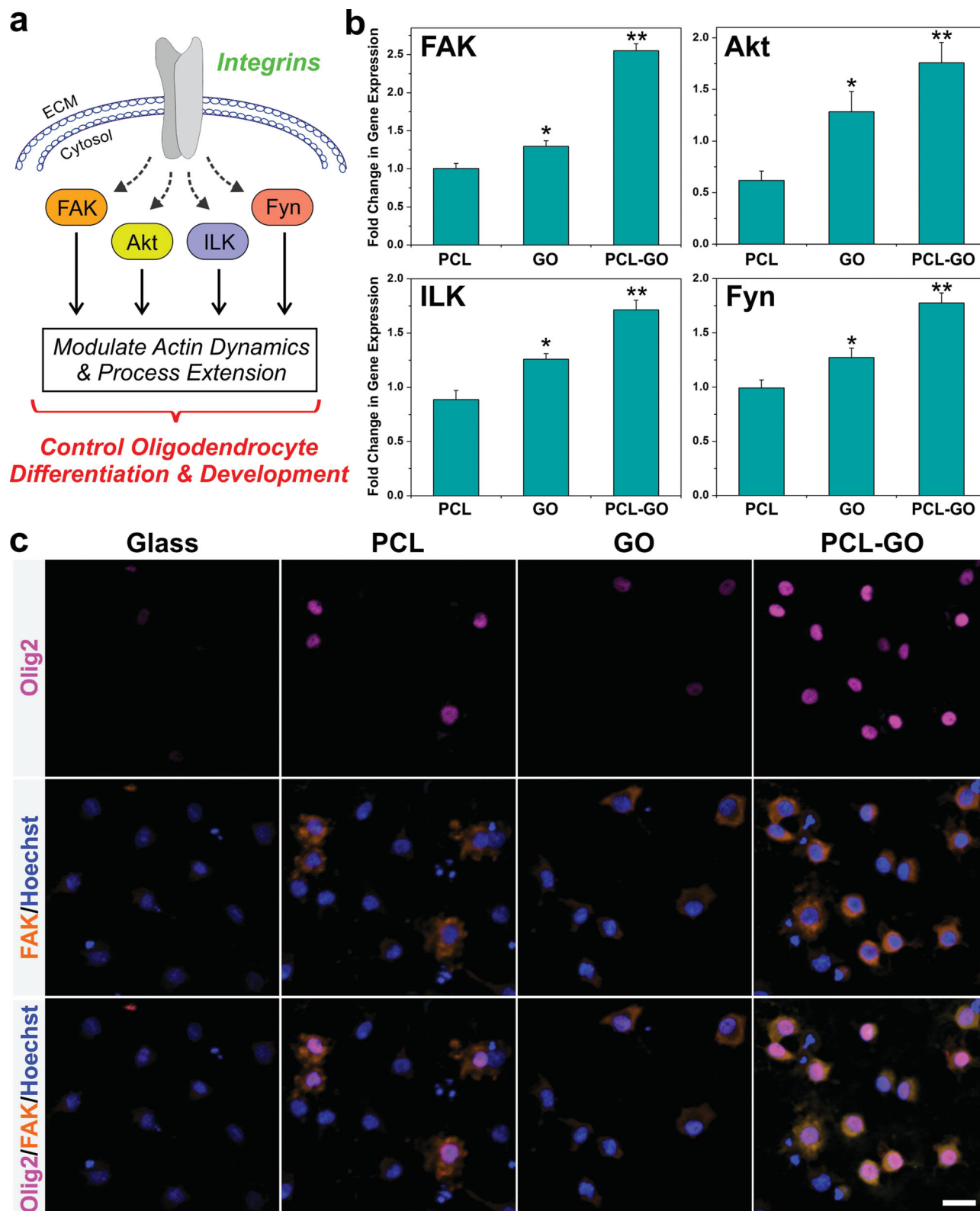


Figure 5. Expression of integrin-related signaling proteins on nanofibrous scaffolds. a) Schematic diagram depicting the integrin signaling proteins involved in oligodendrocyte differentiation and development. b) Quantitative PCR analysis was used to assess the gene expression of the integrin signaling proteins FAK, Akt, ILK and Fyn. The gene expression is relative to GAPDH, and normalized to the conventional PLL-coated glass control. A student's unpaired t-test was used for evaluating the significance ($* = p < 0.05$, $** = p < 0.01$), compared to the PLL-coated glass control. c) Confocal images of NSCs grown on various substrates (PLL-coated glass, PCL only, GO-coated glass and PCL-GO) after six days of culture, co-stained for Olig2 (purple) and FAK (orange). Scale bar: 20 μm .

as survival, differentiation and myelination.^[18] Culminating evidence from previous reports suggests the role of several key signaling proteins downstream of integrins in regulating oligodendrocyte differentiation and development, including focal adhesion kinase (FAK), Akt, integrin-linked kinase (ILK) and Fyn kinase (Fyn)^[18] (Figure 5a). Therefore, we investigated whether oligodendrocyte differentiation-related signal transduction is promoted in NSCs cultured on PCL-GO.

Among the various cell-signaling proteins, we examined the expression of FAK, Akt, ILK and Fyn, which have been found to mediate cytoskeletal remodeling and process extension during oligodendrocyte development. Moreover, disruption of each of these proteins has been reported to cause a variety of developmental defects, including reduced process extension, aberrant myelin formation and attenuated expression of myelin proteins.^[19] We found that NSCs cultured on the GO-coated surfaces enhanced the gene expression of all of these factors (Figure 5b). These signaling molecules exhibited the same trend in expression, wherein the GO-coated glass showed higher expression than PCL, and PCL-GO showed the strongest level of expression with a 2.6-fold increase in FAK and about a 1.7-fold increase in Akt, ILK and Fyn (Figure 5b). Additionally, treating the cells grown on PCL-GO scaffolds with cell signaling inhibitors showed a significant decrease in gene expression of mature oligodendrocyte markers, which provides further evidence for the potential role of such cellular signaling in the observed oligodendrocyte differentiation (Figure S11, Supporting Information). Collectively, this data supports the role of GO-coating in the upregulation of these downstream molecules in the integrin signaling pathway and may explain, at least in part, the enhanced oligodendrocyte differentiation of NSCs on our hybrid scaffolds.

In order to further elucidate this correlation, we sought to observe cellular co-localization of markers indicative of both integrin signaling and oligodendrocyte differentiation using confocal microscopy. Dual staining was carried out for: i) Olig2, an oligodendrocyte marker, and ii) FAK, one of the main regulators of integrin-ECM signaling^[19d] and found in our study to show the highest expression in cells cultured on PCL-GO. The immunostaining for Olig2 (purple) and FAK (orange) was compared for NSCs cultured on PCL-GO with the other control substrates (Figure 5c). As observed earlier, cells grown on PCL-GO showed the strongest intensity and highest number of cells expressing Olig2, with minimal expression on the glass control and moderate expression on PCL and GO. A similar trend was also observed in FAK staining, which corresponds to the gene expression levels shown in Figure 5b. Since the localization of FAK is in the cytoplasm and Olig2 is in the nucleus, the co-localization of the two markers within the same cell can be easily visualized. Interestingly, the cells expressing FAK also expressed Olig2, a phenomenon that was observed on all substrates (Figure 5c). Moreover, PCL-GO showed the strongest expression of both markers and the highest number of cells co-expressing FAK and Olig2. Together, our data suggests that the GO-coating on the nanofiber scaffolds may promote oligodendrocyte differentiation through specific microenvironmental interactions which activate integrin-related intracellular signaling.

Overall, we have demonstrated the capability of a unique graphene-nanofiber hybrid scaffold to provide instructive physical

cues that lead to the selective differentiation of neural stem cells into mature oligodendrocytes, without introducing differentiation inducers in the culture media. The ability to selectively guide stem cell differentiation by merely changing the properties of an underlying biomaterial scaffold is a valuable approach for tissue engineering, which can help complement or potentially eliminate the use of exogenous differentiation inducers such as viral gene vectors, growth factors and small molecule drugs. Moreover, our hybrid scaffold is exceptional in that it combines the well-established properties of nanofibers and graphene-based nanomaterials. For instance, nanofibers have been shown to provide ideal topography for fabricating nerve guidance conduits, directing neurite outgrowth and promoting axonal regeneration.^[3a,11] On the other hand, graphene-based nanomaterials provide permissive surfaces for protein and cell adhesion, as well as high conductivity to mediate electrical stimulation for supporting neuronal electrophysiology.^[20] In turn, a hybrid scaffold which combines the morphological features of nanofibers and the unique surface properties of graphene-based nanomaterials in a single culture platform, can be highly beneficial. We envision that such a platform can serve as a powerful tool for developing future therapies for CNS-related diseases and injuries.

Supporting Information

Supporting Information is available from the Wiley Online Library or from the author.

Acknowledgements

K.-B.L. acknowledges financial support from the NIH Director's Innovator Award [1DP20D006462-01], National Institute of Biomedical Imaging and Bioengineering of the NIH [1R21NS085569-01], the N.J. Commission on Spinal Cord grant [09-3085-SCR-E-0], and the Rutgers Faculty Research Grant Program. S.S. acknowledges NSF DGE 0801620, Integrative Graduate Education and Research Traineeship (IGERT) on the Integrated Science and Engineering of Stem Cells. T.M.U. acknowledges financial support from FAPESP (Research Foundation from São Paulo State) and Prof. Valtencir Zucolotto (University of São Paulo, Brazil). We acknowledge NIH grant S10RR025424 to Dr. Nilgun Tumer for a confocal microscope. The authors acknowledge NSF grant DMR 1126468 to Prof. Torgny Gustafsson and assistance from Dr. Samir Shubeita for helium ion microscope imaging.

Received: February 1, 2014

Revised: February 17, 2014

Published online: March 26, 2014

- [1] a) J. W. McDonald, X. Z. Liu, Y. Qu, S. Liu, S. K. Mickey, D. Turetsky, D. I. Gottlieb, D. W. Choi, *Nat. Med.* **1999**, *5*, 1410; b) S. Pluchino, A. Quattrini, E. Brambilla, A. Gritti, G. Salani, G. Dina, R. Galli, U. Del Carro, S. Amadio, A. Bergami, R. Furlan, G. Comi, A. L. Vescevi, G. Martino, *Nature* **2003**, *422*, 688; c) L. R. Zhao, W. M. Duan, M. Reyes, C. D. Keene, C. M. Verfaillie, W. C. Low, *Exp. Neurol.* **2002**, *174*, 11.
- [2] T. Shindo, Y. Matsumoto, Q. Wang, N. Kawai, T. Tamiya, S. Nagao, *J. Med. Invest.* **2006**, *53*, 42.
- [3] a) H. Cao, T. Liu, S. Y. Chew, *Adv. Drug Delivery Rev.* **2009**, *61*, 1055; b) G. Orive, E. Anitua, J. L. Pedraz, D. F. Emerich, *Nat. Rev. Neurosci.* **2009**, *10*, 682.

- [4] a) H. S. Keirstead, G. Nistor, G. Bernal, M. Totoiu, F. Cloutier, K. Sharp, O. Steward, *J. Neurosci.* **2005**, *25*, 4694; b) M. Abematsu, K. Tsujimura, M. Yamano, M. Saito, K. Kohno, J. Kohyama, M. Namihira, S. Komiya, K. Nakashima, *J. Clin. Invest.* **2010**, *120*, 3255.
- [5] a) S. Y. Park, J. Park, S. H. Sim, M. G. Sung, K. S. Kim, B. H. Hong, S. Hong, *Adv. Mater.* **2011**, *23*, H263; b) S. Shah, A. Solanki, P. K. Sasmal, K.-B. Lee, *J. Am. Chem. Soc.* **2013**, *135*, 15682; c) A. Solanki, S. Shah, P. T. Yin, K.-B. Lee, *Sci. Rep.* **2013**, *3*, 1553; d) J. Takahashi, T. D. Palmer, F. H. Gage, *J. Neurobiol.* **1999**, *38*, 65; e) A. Solanki, S. Shah, K. A. Memoli, S. Y. Park, S. Hong, K.-B. Lee, *Small* **2010**, *6*, 2509.
- [6] F. Sher, R. Rößler, N. Brouwer, V. Balasubramanian, E. Boddeke, S. Copray, *STEM CELLS* **2008**, *26*, 2875; DOI: 10.1634/stemcells.2008-0121.
- [7] F. Sher, V. Balasubramanian, E. Boddeke, S. Copray, *Curr. Opin. Neurol.* **2008**, *21*, 607.
- [8] C. Zhao, A. Tan, G. Pastorin, H. K. Ho, *Biotechnol. Adv.* **2013**, *31*, 654.
- [9] a) Y. Zhu, S. Murali, W. Cai, X. Li, J. W. Suk, J. R. Potts, R. S. Ruoff, *Adv. Mater.* **2010**, *22*, 3906; b) T. H. Kim, K. B. Lee, J. W. Choi, *Biomaterials* **2013**, *34*, 8660.
- [10] a) G. Y. Chen, D. W. Pang, S. M. Hwang, H. Y. Tuan, Y. C. Hu, *Biomaterials* **2012**, *33*, 418; b) W. C. Lee, C. H. Lim, H. Shi, L. A. Tang, Y. Wang, C. T. Lim, K. P. Loh, *ACS Nano* **2011**, *5*, 7334; c) A. Solanki, S.-T. D. Chueng, P. T. Yin, R. Kappera, M. Chhowalla, K.-B. Lee, *Adv. Mater.* **2013**, *25*, 5477.
- [11] J. Xie, M. R. MacEwan, A. G. Schwartz, Y. Xia, *Nanoscale* **2010**, *2*, 35.
- [12] A. Cipitria, A. Skelton, T. R. Dargaville, P. D. Dalton, D. W. Huttmacher, *J. Mater. Chem.* **2011**, *21*, 9419.
- [13] G. T. Christopherson, H. Song, H. Q. Mao, *Biomaterials* **2009**, *30*, 556.
- [14] Q. Shen, Y. Wang, E. Kokovay, G. Lin, S. M. Chuang, S. K. Goderie, B. Roysam, S. Temple, *Cell Stem Cell* **2008**, *3*, 289.
- [15] N. Baumann, D. Pham-Dinh, *Physiol. Rev.* **2001**, *81*, 871.
- [16] a) S. Lee, M. K. Leach, S. A. Redmond, S. Y. Chong, S. H. Mellon, S. J. Tuck, Z. Q. Feng, J. M. Corey, J. R. Chan, *Nat. Methods* **2012**, *9*, 917; b) D. R. Nisbet, L. M. Yu, T. Zahir, J. S. Forsythe, M. S. Shoichet, *J. Biomater. Sci., Polym. Ed.* **2008**, *19*, 623.
- [17] H. Colognato, I. D. Tzvetanova, *Dev. Neurobiol.* **2011**, *71*, 924.
- [18] R. W. O'Meara, J. P. Michalski, R. Kothary, *J. Signal Transduction* **2011**, *2011*, 354091.
- [19] a) R. W. O'Meara, J. P. Michalski, C. Anderson, K. Bhanot, P. Rippstein, R. Kothary, *J. Neurosci.* **2013**, *33*, 9781; b) D. J. Osterhout, A. Wolven, R. M. Wolf, M. D. Resh, M. V. Chao, *J. Cell Biol.* **1999**, *145*, 1209; c) C. S. Barros, T. Nguyen, K. S. Spencer, A. Nishiyama, H. Colognato, U. Muller, *Development* **2009**, *136*, 2717; d) A. D. Forrest, H. E. Beggs, L. F. Reichardt, J. L. Dupree, R. J. Colello, B. Fuss, *J. Neurosci. Res.* **2009**, *87*, 3456.
- [20] Y. Zhang, T. R. Nayak, H. Hong, W. Cai, *Nanoscale* **2012**, *4*, 3833.